26. Neutrinos in Cosmology

Revised August 2023 by J. Lesgourgues (TTK, RWTH) and L. Verde (ICC, U. of Barcelona; ICREA, Barcelona).

26.1 Standard neutrino cosmology

Neutrinos leave detectable imprints on cosmological observations that can then be used to constrain neutrino properties. This is a great example of the remarkable interconnection and interplay between nuclear physics, particle physics, astrophysics and cosmology (for general reviews see *e.g.*, [1–4]). Present cosmological data are already providing constraints on neutrino properties not only complementary but also competitive with terrestrial experiments; for instance, upper bounds on the total neutrino mass have shrinked by a factor of about 20 in the past two decades. Forthcoming cosmological data may soon provide key information, not obtainable in other ways like *e.g.*, a measurement of the absolute neutrino mass scale.

A relic neutrino background pervading the Universe (the Cosmic Neutrino background, CνB) is a generic prediction of the standard hot Big Bang model (see Big Bang Nucleosynthesis – Chap. 24 of this *Review*). While it has not yet been detected directly, it has been indirectly confirmed by the accurate agreement of predictions and observations of: *a*) the primordial abundance of light elements (see Big Bang Nucleosynthesis – Chap. 24) of this *Review*; *b*) the power spectrum of Cosmic Microwave Background (CMB) anisotropies (see Cosmic Microwave Background – Chap. 29 of this *Review*); and *c*) the large-scale clustering of cosmological structures. Within the hot Big Bang model such good agreement would fail dramatically without a CνB with properties matching closely those predicted by the standard neutrino decoupling process (*i.e.*, involving only weak interactions).

We will illustrate below that cosmology is sensitive to the following neutrino properties: their density, related to the number of active (*i.e.*, left-handed, see Neutrino Mass, Mixing, and Oscillations - Chap. 14 of this *Review*) neutrino species, and their masses. At first order, cosmology is sensitive to the total neutrino mass, but is blind to the mixing angles and CP violation phase as discussed in Neutrino Mass, Mixing, and Oscillations (Chap. 14 of this *Review*). This makes cosmological constraints nicely complementary to measurements from terrestrial neutrino experiments.

The minimal cosmological model, ΛCDM, currently providing a good fit to most cosmological data sets (with the exception of some data in tension, discussed in The Cosmological Parameters Chap. 25 of this *Review*), assumes that the only massless or light (sub-keV) relic particles since the Big Bang Nucleosynthesis (BBN) epoch are photons and active neutrinos. Extended models with light sterile neutrinos, light thermal axions or other light relics –sometimes referred to as "dark radiation"– would produce effects similar to, and potentially degenerate with, those of active neutrinos. Thus neutrino bounds are often discussed together with limits on such scenarios. In case of anomalies in cosmological data, it might not be obvious to discriminate between interpretation in terms of active neutrinos with non-standard decoupling, additional production mechanisms, non-standard interactions, etc., or in terms of some additional light particles. Such extensions have been explored as a possible way to resolve the H_0 tension between late and early Universe determinations [5–8], but are not widely favoured [9–11].

Hence neutrino density and mass bounds can be derived under the assumption of no additional massless or light relic particles, and the neutrino density measured in that way provides a test of standard (*i.e.*, involving only weak interactions) neutrino decoupling.

In that model, the three active neutrino types thermalize in the early Universe, with a negligible leptonic asymmetry. Then they can be viewed as three propagating mass eigenstates sharing the

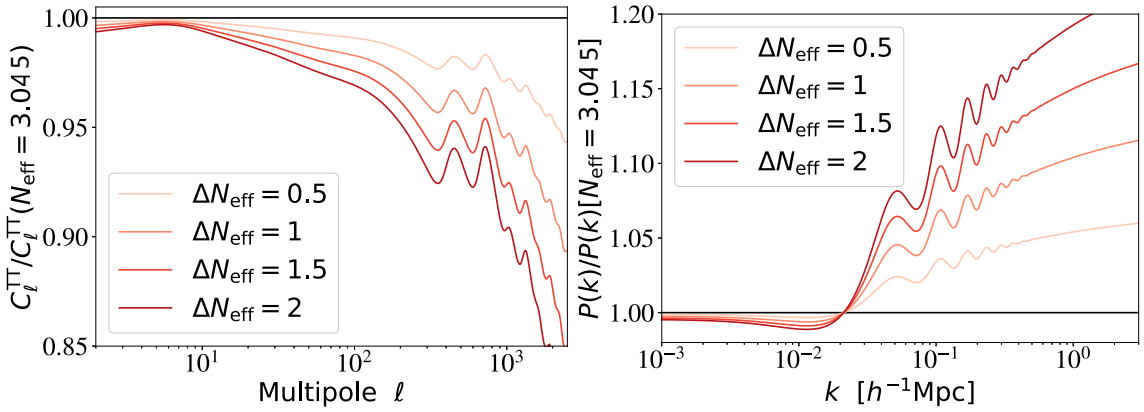

Figure 26.1: Ratio of the CMB C_ℓ^{TT} (left, including lensing effects) and matter power spectrum $P(k)$ (right, computed for each model in units of $(h^{-1}\mathrm{Mpc})^3$) for different values of $\Delta N_{\rm eff} \equiv N_{\rm eff} - 3.044$ over those of a reference model with $\Delta N_{\rm eff} = 0$. In order to minimize and better characterise the effect of $N_{\rm eff}$ on the CMB, the parameters that are kept fixed are $\{z_{\rm eq},\ z_\Lambda,\ \omega_{\rm b},\ \tau\}$ and the primordial spectrum parameters. Fixing $\{z_{\rm eq},\ z_\Lambda\}$ is equivalent to fixing the fractional density of total radiation, of total matter and of cosmological constant $\{\Omega_{\rm r}, \Omega_{\rm m}, \Omega_\Lambda\}$ while increasing the Hubble parameter as a function of $N_{\rm eff}$. The statistical errors on the C_ℓ are $\sim 1\%$ for a band power of $\Delta\ell = 30$ at $\ell \sim 1000$. The error on $P(k)$ is estimated to be of the order of 5%.

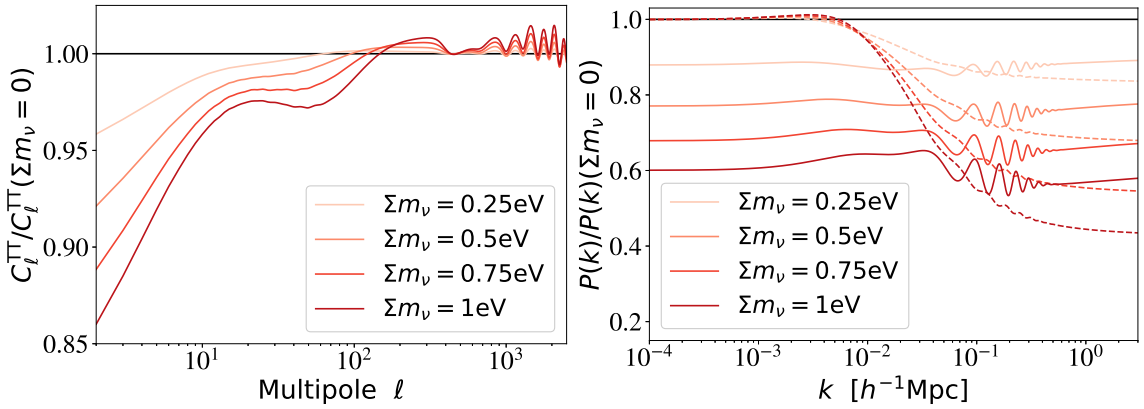

Figure 26.2: Ratio of the CMB C_ℓ^{TT} and matter power spectrum $P(k)$ (computed for each model in units of $(h^{-1}\mathrm{Mpc})^3$) for different values of $\sum m_\nu$ over those of a reference model with massless neutrinos. In order to minimize and better characterise the effect of $\sum m_\nu$ on the CMB, the parameters that are kept fixed are $\omega_{\rm b}$, $\omega_{\rm c}$, τ, the angular scale of the sound horizon $\theta_{\rm s}$ and the primordial spectrum parameters (solid lines). This implies that we are increasing the Hubble parameter h as a function of $\sum m_\nu$. For the matter power spectrum, in order to single out the effect of neutrino free-streaming on $P(k)$, the dashed lines show the spectrum ratio when $\{\omega_{\rm m}, \omega_{\rm b}, \Omega_\Lambda\}$ are kept fixed. For comparison, the error on $P(k)$ is of the order of 5% with current observations, and the fractional C_ℓ errors are of the order of $1/\sqrt{\ell}$ at low ℓ.

same temperature and identical Fermi-Dirac distributions, thus with no visible effects of flavour oscillations. Neutrinos decouple gradually from the thermal plasma at temperatures $T \sim 2\,\mathrm{MeV}$. In the instantaneous neutrino decoupling limit, *i.e.*, assuming that neutrinos were fully decoupled at the time when electron-positrons annihilate and release entropy in the thermal bath, the neutrino-

to-photon density ratio between the time of electron-positron annihilation and the non-relativistic transition of neutrinos would be given by

$$\frac{\rho_\nu}{\rho_\gamma} = \frac{7}{8} N_{\rm eff} \left(\frac{4}{11}\right)^{4/3} , \tag{26.1}$$

with $N_{\rm eff} = 3$, and the last factor comes from the fourth power of the temperature ratio $T_\nu/T_\gamma = (4/11)^{1/3}$ (see Big Bang Cosmology – Chap. 22 in this *Review*). In the above formula, $N_{\rm eff}$ is called the effective number of neutrino species because it can be viewed as a convenient parametrisation of the relativistic energy density of the Universe beyond that of photons, in units of one neutrino in the instantaneous decoupling limit. Precise simulations of neutrino decoupling and electron-positron annihilation, taking into account flavor oscillations, provide precise predictions for the actual phase-space distribution of relic neutrinos [12–18]. These distributions differ from the instantaneous decoupling approximation through a combination of a small shift in the photon temperature and small flavor-dependent non-thermal distortions, all at the percent level. The final result for the density ratio ρ_ν/ρ_γ in the relativistic regime can always be expressed as in Eq. (26.1), but with a different value of $N_{\rm eff}$. The most recent analyses, that includes the effect of neutrino oscillations with the present values of the mixing parameters, an improved calculation of the collision terms and the most recent results on plasma thermodynamics QED corrections, give[1] $N_{\rm eff} = 3.044$ [16, 17]. The precise number density ratio n_ν/n_γ can also be derived from such studies, and is important for computing the ratio $\Omega_\nu h^2/\sum_i m_i$ (ratio of the physical density of neutrinos in units of the critical density to the sum of neutrino masses) in the non-relativistic regime. Once neutrinos are decoupled, their momentum redshifts like $p \propto 1/a$ but, due to the absence of interactions, their phase-space distributions remain constant when expressed in terms of the comoving momentum $q = pa$, even when they become non-relativistic.

The neutrino temperature today, $T_\nu^0 \simeq 1.7 \times 10^{-4}\,{\rm eV} \simeq 1.9\,{\rm K}$, is smaller than at least two of the neutrino masses, since the two squared-mass differences are $|\Delta m^2_{31}|^{1/2} > |\Delta m^2_{21}|^{1/2} > T_\nu^0$ (see Neutrino mass, Mixing, and oscillations – Chap. 14 of this *Review*). Thus at least two neutrino mass eigenstates are non-relativistic today and behave as a small "hot" fraction of the total dark matter (they cannot be all the dark matter, as explained in Chap. 27 in this *Review*). This fraction of hot dark matter can be probed by cosmological experiments, for two related reasons, as we now describe.

First, neutrinos are the only known particles behaving as radiation at early times (during the CMB acoustic oscillations) and dark matter at late times (during structure formation), which has consequences on the background evolution. Neutrinos become non-relativistic when their mass is equal to their average momentum, given for any Fermi-Dirac-distributed particle by $\langle p \rangle = 3.15\,T$. Thus the redshift of the non-relativistic transition is given by $z_i^{\rm nr} = m_i/(3.15\,T_\nu^0) - 1 = m_i/[0.53\,{\rm meV}] - 1$ for each eigenstate of mass m_i, giving for instance $z_i^{\rm nr} = 110$ for $m_i = 60\,{\rm meV}$, corresponding to a time deep inside the matter-dominated regime. Second, until the non-relativistic transition, neutrinos travel at the speed of light, and later on they move at a typical velocity $\langle v_i/c \rangle = 3.15\,T_\nu(z)/m_i = 0.53(1+z)\,{\rm meV}/m_i$, which is several orders of magnitude larger than that of the dominant cold (or even of possibly warm) dark matter component(s). This brings their characteristic diffusion scale, called the "free-streaming length", to cosmological relevant values, with consequences on gravitational clustering and the growth of structure.

Once neutrinos are non-relativistic, their energy density is given by $\rho_\nu \simeq \sum m_i n_i$. Since the number densities n_i are equal to each other (up to negligible corrections coming from flavour effects in the decoupling phase), the total mass $\sum m_\nu = m_1 + m_2 + m_3$ can be factorized out. It is

[1] The last effects that potentially require some further checks in order to fully settle the fourth significant digit in $N_{\rm eff}$ are temperature QED corrections; according to [18], the final result might be closer to 3.043 than to 3.044.

possible that the lightest neutrino is still relativistic today, in which case this relation is slightly incorrect, but given that the total density is always strongly dominated by that of non-relativistic neutrinos, the error made is completely negligible. Using the expression for n_i/n_γ obtained from precise neutrino decoupling studies [16, 17], and knowing n_γ from the measurement of the CMB temperature, one can compute ρ_ν^0, the total neutrino density today,[2] in units of the critical density $\rho_{\rm crit}^0$:

$$\Omega_\nu = \frac{\rho_\nu^0}{\rho_{\rm crit}^0} = \frac{\sum m_\nu}{93.12 h^2\,{\rm eV}}\,, \tag{26.2}$$

and the total neutrino average number density today: $n_\nu^0 = 339.5$ cm^{-3} [19]. Here h is the Hubble constant in units of 100 km s^{-1} Mpc^{-1}.

26.2 Effects of neutrino properties on cosmological observables

As long as they are relativistic, *i.e.*, until some time deep inside the matter-dominated regime for neutrinos with a mass $m_i \ll 3.15\,T_\nu^{\rm eq} \sim 1.5\,$eV (see Big Bang Cosmology, Chap. 22 in this *Review*), neutrinos enhance the density of radiation: this effect is parameterised by $N_{\rm eff}$ and can be discussed separately from the effect of the mass that will be described later in this section. Increasing $N_{\rm eff}$ impacts the observable spectra of CMB anisotropies and matter fluctuations through background and perturbation effects.

26.2.1 *Effect of $N_{\rm eff}$ on the CMB*

The background effects depend on what is kept fixed when increasing $N_{\rm eff}$. If the densities of other species are kept fixed, a higher $N_{\rm eff}$ implies a smaller redshift of radiation-to-matter equality, with very strong effects on the CMB spectrum: when the amount of expansion between radiation-to-matter equality and photon decoupling is larger, the CMB peaks are suppressed. This effect is not truly characteristic of the neutrino density, since it can be produced by varying several other parameters. Hence, to characterise the effect of $N_{\rm eff}$, it is more useful and illuminating to enhance the density of total radiation, of total matter and of Λ by exactly the same amount, in order to keep the redshift of radiation-to-matter equality $z_{\rm eq}$ and matter-to-Λ equality z_Λ fixed [20–22]. The primordial spectrum parameters, the baryon density $\omega_{\rm b} \equiv \Omega_{\rm b} h^2$ and the optical depth to reionization τ can be kept fixed at the same time, since we can simply vary $N_{\rm eff}$ together with the Hubble parameter h with fixed $\{\omega_{\rm b},\, \Omega_{\rm c},\, \Omega_\Lambda\}$. The impact of such a transformation is shown in Fig. 26.1 for the CMB temperature spectrum C_ℓ^{TT} (defined in Chap. 29 in this *Review*) and for the matter power spectrum $P(k)$ (defined in Chap. 22 in this *Review*) for several representative values of $N_{\rm eff}$. These effects are within the reach of cosmological observations given current error bars, as discussed in Section 26.3.1 (for instance, with the *Planck* satellite data, the statistical error on the C_ℓ's is of the order of one per cent for a band power of $\Delta\ell = 30$ at $\ell \sim 1000$).

With this transformation, the main background effect of $N_{\rm eff}$ is an increase in the diffusion scale (or Silk damping scale, see Cosmic Microwave Background – Chap. 29 in this *Review*) at the time of decoupling, responsible for the decrease in C_ℓ^{TT} at high ℓ, plus smaller effects coming from a slight increase in the redshift of photon decoupling [20–22]. At the level of perturbations, a higher $N_{\rm eff}$ implies that photons feel gravitational forces from a denser neutrino component; this tends to decrease the acoustic peaks (because neutrinos are distributed in a smoother way than photons) and to shift them to larger scales / smaller multipoles (because photon perturbations traveling at the speed of sound in the photon-baryon fluid feel some dragging effect from neutrino perturbations travelling at the speed of light) [20,22,23]. The effect of increasing $N_{\rm eff}$ on the polarization spectrum features are the same as on the temperature spectrum: an increased Silk damping, and a shift in

[2] The value 93.12 eV applies to the limit of large masses, in which $\rho_\nu^0 = \sum m_i n_i^0$ and neutrinos are degenerate in mass [19]. This number would be larger by ∼0.1% in the limit of minimal normal hierarchy (or smaller by ∼0.06% for minimal inverted hierarchy), due the lighest mass state(s) being still relativistic today and to flavor-dependent non-thermal distortions in the neutrino phase-space distributions.

the acoustic peak amplitude and location - the latter effect is even more clear in the polarization spectrum, in which the location of acoustic peaks does not get further influenced by a Doppler effect like for temperature. The combination of these effects is truly characteristic of the radiation density parameter $N_{\rm eff}$ and cannot be mimicked by other parameters; thus $N_{\rm eff}$ can be accurately measured from the CMB alone. However, there are correlations between $N_{\rm eff}$ and other parameters. In particular, we have seen (Fig. 26.1) that in order to minimise the effect of $N_{\rm eff}$ on the CMB spectrum, one should vary h at the same time, hence there is a correlation between $N_{\rm eff}$ and h, which implies that independent measurements reducing the error bar on h also reduce that on $N_{\rm eff}$. Note that this correlation is not equivalent to a perfect degeneracy, so both parameters can be constrained with CMB data alone.

Table 26.1: Summary of $N_{\rm eff}$ constraints.

	Model	$N_{\rm eff}$	Ref.
CMB alone			
Pl18[TT,TE,EE+lowE]	ΛCDM+$N_{\rm eff}$	$2.92^{+0.36}_{-0.37}$ (95%CL)	[24]
CMB + background evolution + LSS			
Pl18[TT,TE,EE+lowE+lensing] + BAO	ΛCDM+$N_{\rm eff}$	$2.99^{+0.34}_{-0.33}$ (95%CL)	[24]
"	" +5-params.	$2.85^{+0.23}_{-0.23}$ (68%CL)	[25]

26.2.2 *Effect of $N_{\rm eff}$ on the matter spectrum*

We have discussed the effect of increasing $N_{\rm eff}$ while keeping $z_{\rm eq}$ and $\omega_{\rm b}$ fixed, because the latter two quantities are very accurately constrained by CMB data. This implies that $\omega_{\rm c}$ increases with $N_{\rm eff}$, and that the ratio $\omega_{\rm b}/\omega_{\rm c} = \Omega_{\rm b}/\Omega_{\rm c}$ decreases. However, the ratio of baryonic-to-dark matter has a strong impact on the shape of the matter power spectrum, because until the time of decoupling of the baryons from the photons, CDM experiences gravitational collapse, while baryons are kept smoothly distributed by photon pressure and affected by acoustic oscillations. The decrease of $\Omega_{\rm b}/\Omega_{\rm c}$ following from the increase of $N_{\rm eff}$ gives more weight to the most clustered of the two components, namely the dark matter one, and produces an enhancement of the small-scale matter power spectrum and a damping of the amplitude of baryon acoustic oscillations (BAOs), clearly visible in Fig. 26.1 (right plot). The scale of BAOs is also slightly shifted by the same neutrino dragging effect as for CMB peaks [20, 26].

The increase in the small-scale matter power spectrum is also responsible for a last effect on the CMB spectra: the CMB last scattering surface is slightly more affected by weak lensing from large-scale structures. This tends to smooth the maxima, the minima, and the damping scale of the CMB spectra [27].

26.2.3 *Effect of neutrino masses on the CMB*

Neutrino eigenstates with a mass $m_i \ll 0.6\,{\rm eV}$ become non-relativistic after photon decoupling. They contribute to the non-relativistic matter budget today, but not at the time of equality or recombination. If we increase the neutrino mass while keeping fixed the density of baryons and dark matter ($\omega_{\rm b}$ and $\omega_{\rm c}$), the early cosmological evolution remains fixed and independent of the neutrino mass, until the time of the non-relativistic transition. Thus one might expect that the CMB temperature and polarization power spectra are left invariant. This is not true for four reasons.

First, the neutrino density enhances the total non-relativistic density at late times, $\omega_{\rm m} = \omega_{\rm b} + \omega_{\rm c} + \omega_\nu$, where $\omega_\nu \equiv \Omega_\nu h^2$ is given as a function of the total mass $\sum m_\nu$ by Eq. (26.2). The late background evolution impacts the CMB spectrum through the relation between scales

on the last scattering surface and angles on the sky, and through the late ISW effect (see Cosmic Microwave Background – Chap. 29 of this *Review*). These two effects depend respectively on the angular diameter distance to recombination, $d_A(z_{\rm rec})$, and on the redshift of matter-to-Λ equality. Increasing $\sum m_\nu$ tends to modify these two quantities. By playing with h and Ω_Λ, it is possible to keep one of them fixed, but not both at the same time. Since the CMB measures the angular scale of acoustic oscillations with exquisite precision, and is only loosely sensitive to the late ISW effect due to cosmic variance, we choose in Fig. 26.2 to play with the Hubble parameter in order to maintain a fixed scale $d_A(z_{\rm rec})$. With such a choice, an increase in neutrino mass comes together with a decrease in the late ISW effect explaining the depletion of the CMB spectrum for $l \leq 20$. The fact that both $\sum m_\nu$ and h enter the expression of $d_A(z_{\rm rec})$ implies that measurements of the neutrino mass from CMB data are strongly correlated with h. Second, the non-relativistic transition of neutrinos affects the total pressure-to-density ratio of the Universe, and causes a small variation of the metric fluctuations. If this transition takes place not too long after photon decoupling, this variation is observable through the early ISW effect [22, 28, 29]. It is responsible for the dip seen in Fig. 26.2 for $20 \leq \ell \leq 200$. Third, when the neutrino mass is higher, the CMB spectrum is less affected by the weak lensing effect induced by the large-scale structure at small redshift. This is due to a decrease in the matter power spectrum described in the next paragraphs. This reduced lensing effect is responsible for most of the oscillatory patterns visible in Fig. 26.2 (left plot) for $\ell \geq 200$. Fourth, the neutrinos with the smallest momenta start to be non-relativistic earlier than the average ones. The photon perturbations feel this through their gravitational coupling with neutrinos. This leads to a small enhancement of C_l^{TT} for $\ell \geq 500$, hardly visible on Fig. 26.2 because it is balanced by the lensing effect.

26.2.4 *Effect of neutrino masses on the matter spectrum*

The physical effect of neutrinos on the matter power spectrum is related to their velocity dispersion. Neutrinos free-stream over large distances without falling into small potential wells. The free-streaming scale is roughly defined as the distance travel by neutrinos over a Hubble time scale $t_{\rm H} = (a/\dot{a})$, and approximates the scale below which neutrinos remain very smooth. On larger scales, they cluster in the same way as cold dark matter. The power spectrum of total matter fluctuations, related to the squared fluctuation $\delta_{\rm m}^2$ with $\delta_{\rm m} \equiv \delta_{\rm b} + \delta_{\rm c} + \delta_\nu$, gets a negligible contribution from the neutrino component on small scales, and is reduced by a factor $(1 - 2f_\nu)$, where $f_\nu = \omega_\nu/\omega_{\rm m}$. Additionally, on scales below the free-streaming scale, the growth of ordinary cold dark matter and baryon fluctuations is modified by the fact that neutrinos contribute to the background density, but not to the density fluctuations. This changes the balance between the gravitational forces responsible for clustering, and the Hubble friction term slowing it down. Thus the growth rate of CDM and baryon fluctuations is reduced [30]. This results today in an additional suppression of the small-scale linear matter power spectrum by approximately $(1 - 6f_\nu)$. These two effects sum up to a factor $(1 - 8f_\nu)$ [31] (more precise approximations can be found in [2, 22]). The non-linear spectrum is even more suppressed on mildly non-linear scales [3, 32–36].

This effect is often illustrated by plots of the matter power spectrum ratio with fixed parameters $\{\omega_{\rm m}, \omega_{\rm b}, \Omega_\Lambda\}$ and varying f_ν, *i.e.*, with the CDM density adjusted to get a fixed total dark matter density [2, 22, 31] (see Fig. 26.2, right plot, dashed lines). This transformation does not leave the redshift of equality $z_{\rm eq}$ invariant, and has very large effects on the CMB spectra. If one follows the logic of minimizing CMB variations and fixing $z_{\rm eq}$ like in the previous paragraphs, the increase in $\sum m_\nu$ must take place together with an increase of h, which tends to suppress the large-scale power spectrum, by approximately the same amount as the neutrino free-streaming effect [37]. In that case, the impact of neutrino masses on the matter power spectrum appears as an overall amplitude suppression, which can be seen in Fig. 26.2 (right plot, solid lines). The oscillations

on intermediate wavenumbers come from a small shift in the BAO scale [37]. This global effect is not degenerate with a variation of the primordial spectrum amplitude $A_{\rm s}$, because it only affects the matter power spectrum, and not the CMB spectra. However, the amplitude of the CMB temperature and polarization spectrum is given by the combination $A_{\rm s}e^{-2\tau}$. Hence a measurement of τ is necessary in order to fix $A_{\rm s}$ from CMB data, and avoid a parameter degeneracy between $\sum m_\nu$ and $A_{\rm s}$ [37–39].

A few of the neutrino mass effects described above –free-streaming scale, early ISW– depend on individual masses m_i, but most of them depend only on the total mass through f_ν –suppression of the matter power spectrum, CMB lensing, shift in angular diameter distance–. Because the latter effects are easier to measure, cosmology is primarily sensitive to the total mass $\sum m_\nu$ [40, 41]. The possibility that future data sets might be able to measure individual masses or the mass hierarchy, despite systematic errors and parameter degeneracies, an active area of investigation [42–48].

26.3 Cosmological Constraints on neutrino properties

In this review we focus on cosmological constraints on the abundance and mass of ordinary active neutrinos. Several stringent but model-dependent constraints on non-standard neutrinos (*e.g.*, sterile neutrinos, active neutrinos with interactions beyond the weak force, unstable neutrinos with invisible decay, etc.) can also be found in the literature.

We highlight that cosmological constraints on neutrino properties are always obtained within the framework of a ΛCDM model or simple and popular extensions of this model as spelled out in the following subsections. In light of the emergence of cosmological tensions and especially the so-called Hubble tension which has now reached the $\sim 5\sigma$ level (see Chap. 25 of this *Review*), it is important to bear in mind the following considerations. Inconsistent measurements should not be combined: bounds obtained from combination of discrepant data sets should be considered with extreme caution. Additionally, the constraints reported below assume that the solution of the H_0 tension –whatever that may be– leaves the interpretation of the adopted probes unaffected.

26.3.1 *Neutrino abundance*

Table 26.1 shows a list of constraints on $N_{\rm eff}$ obtained with several combination of data sets. 'Pl18' denotes the *Planck* 2018 data, composed of a high-ℓ temperature+polarization likelihood (TT,TE,EE), low-ℓ polarization (low E) and CMB lensing spectrum likelihood (lensing) based on lensing extraction from quadratic estimators [24]. 'BAO' refers to measurements of the BAO scale (and hence of the angular diameter distance) described in detail in the references given in the table.

Within the framework of a 7-parameter cosmological model (ΛCDM+$N_{\rm eff}$), the constraint on $N_{\rm eff}$ from the *Planck* 2018 data release [TT,TE,EE+lowE] is $N_{\rm eff} = 2.92^{+0.36}_{-0.37}$ (95%CL). This number is perfectly compatible with the prediction of the standard neutrino decoupling model, $N_{\rm eff} = 3.044$, and can be viewed as a proof of self-consistency of the cosmological model.

The bounds can be tightened by adding information on the low-redshift background expansion from BAOs. Finally one may also add information from large-scale structure (LSS), *i.e.*, on the growth rate and clustering amplitude of matter as a function of scale, although LSS data are not very constraining for the $N_{\rm eff}$ parameter. The second result quoted in Table 26.1 shows that the $N_{\rm eff}$ bound tightens slightly when adding BAO information from the BOSS galaxy survey plus LSS information from the *Planck* CMB lensing spectrum. Adding more recent data on BAOs and redshift-space distortions (RSDs) from the eBOSS galaxy survey [49] only provides a very marginal improvement of the bounds [54]. All combinations of *Planck* 2018 data with BAO and/or LSS data return measurements consistent with the standard expectation.

The situation is different with the inclusion of low-redshift measurements of H_0 with distance ladders (DLs) [55, 56], now reaching a 5.7σ tension with *Planck* in the ΛCDM framework. As explained in Section 26.2, the positive correlation between $N_{\rm eff}$ and h means that inclusion of the

Table 26.2: Summary of $\sum m_\nu$ constraints.

	Model	95% CL (eV)	Ref.
CMB alone			
Pl18[TT+lowE]	ΛCDM+$\sum m_\nu$	< 0.54	[24]
Pl18[TT,TE,EE+lowE]	ΛCDM+$\sum m_\nu$	< 0.26	[24]
CMB + probes of background evolution			
Pl18[TT,TE,EE+lowE] + BAO	ΛCDM+$\sum m_\nu$	< 0.13	[49]
Pl18[TT,TE,EE+lowE] + BAO	ΛCDM+$\sum m_\nu$+5 params.	< 0.515	[25]
CMB + LSS			
Pl18[TT+lowE+lensing]	ΛCDM+$\sum m_\nu$	< 0.44	[24]
Pl18[TT,TE,EE+lowE+lensing]	ΛCDM+$\sum m_\nu$	< 0.24	[24]
Pl18[TT,TE,EE+lowE]+ ACT[lensing]	ΛCDM+$\sum m_\nu$	< 0.12	[50]
CMB + probes of background evolution + LSS			
Pl18[TT,TE,EE+lowE] + BAO + RSD	ΛCDM+$\sum m_\nu$	< 0.10	[49]
Pl18[TT,TE,EE+lowE+lensing] + BAO + RSD + Shape	ΛCDM+$\sum m_\nu$	< 0.082	[51]
Pl18[TT+lowE+lensing] + BAO + Lyman-α	ΛCDM+$\sum m_\nu$	< 0.087	[52]
Pl18[TT,TE,EE+lowE] + BAO + RSD + SN + DES-Y1	ΛCDM+$\sum m_\nu$	< 0.12	[49]
Pl18[TT,TE,EE+lowE] + BAO + RSD + SN + DES-Y3	ΛCDM+$\sum m_\nu$	< 0.13	[53]

H_0 measurement would tend to push $N_{\rm eff}$ to higher values. However, the high values of $N_{\rm eff}$ that would potentially reconcile the measured CMB or BAO peak scale with the Hubble parameter suggested by DLs, $H_0 \sim 73$ km/s/Mpc, are excluded by the measurement of the damping tail of the CMB temperature spectrum, either by *Planck* itself (given the previously quoted $N_{\rm eff}$ bounds) or by more recent and independent small-scale CMB data sets (as shown e.g. in [57]). Thus, the $N_{\rm eff}$ extension to the ΛCDM model does not reduce the tension significantly, and the combination of *Planck* and DL data does not return any meaningful constraint on $N_{\rm eff}$ in this context. It is currently unclear whether a resolution of the Hubble tension would require a departure from the ΛCDM (or ΛCDM+$N_{\rm eff}$) model [11, 58–62].

As long as DL data are not included, the error bars on $N_{\rm eff}$ degrade mildly when the data are analysed in the context of more extended cosmological scenarios. Adding only the total neutrino mass as an 8th free parameter has a negligible impact on the bounds. The authors of Ref. [25] take a more extreme point of view and fit a 12-parameter model to Pl18[TT,TE,EE+lowE+lensing] data; they obtain $N_{\rm eff} = 2.95 \pm 0.24$ (68% CL), showing that it is very difficult with current cosmological data to accommodate shifts of more than 0.5 from the standard $N_{\rm eff}$ value, and to obtain good fits with, for instance, a fourth (sterile) thermalized neutrino. This is interesting since the anomalies in some oscillation data could be interpreted as evidence for at least one sterile neutrino with a large mixing angle, which would need to be thermalised unless non-standard interactions come into play [5]. In other words, cosmology disfavours the explanation of the oscillations anomalies in terms of extra neutrinos if they are thermalized.

However, if a resolution to the Hubble tension requires a departure from the ΛCDM model or its most simple extensions, the situation is more open. In the presence of new physical ingredients (such as, e.g., non-standard interactions, exotic dark matter candidates, non-minimal dark energy properties or modified gravity), it is in principle conceivable that $N_{\rm eff}$ reaches larger values. However, to date, none of these ingredients has been shown to fully solve the Hubble tension and reconcile CMB, BAO, DL, and supernovae data.

26.3.2 *Are they really neutrinos, as expected?*

While a value of $N_{\rm eff}$ significantly different from zero (at more than 15σ) and consistent with the expected number 3.044 yields a powerful indirect confirmation of the CνB, departures from standard $N_{\rm eff}$ could be caused by any ingredient affecting the early-time expansion rate of the Universe. Extra relativistic particles (either decoupled, self-interacting, or interacting with a dark sector), a background of gravitational waves, an oscillating scalar field with quartic potential, departures from Einstein gravity, or large extra dimensions are some of the possibilities for such ingredients. In principle one could even assume that the cosmic neutrino background never existed or has decayed (like in the "neutrinoless Universe" model of [63]) while another dark radiation component is responsible for $N_{\rm eff}$. At least, cosmological data allow to narrow the range of possible interpretations of $N_{\rm eff} \simeq 3$ to the presence of decoupled relativistic relics like standard neutrinos. Indeed, free-streaming particles leave specific signatures in the CMB and LSS spectra, because their density and pressure perturbations, bulk velocities and anisotropic stress also source the metric perturbations. These signatures can be tested in several ways.

A first approach consists of introducing a self-interaction term in the neutrino equations [6, 7]. Ref. [8] finds that current CMB and BAO data are compatible with no self-interactions. The upper limit to the effective coupling constant $G_{\rm eff}$ for a Fermi-like four-fermions interaction at 95% confidence is $\log_{10}(G_{\rm eff}{\rm MeV}^2) < -1.47$ for Pl18+BAO [11]. Note however that neutrino self-interactions as strong as $\log_{10}(G_{\rm eff}{\rm MeV}^2) \simeq -1.4$ could reconcile CMB temperature and BAO data with the direct H_0 measurement of Ref [64], but such interactions seem to be hardly compatible with BBN, laboratory constraints [10] and CMB polarization [9, 11].

A second approach consists of introducing two phenomenological parameters, $c_{\rm eff}$ and $c_{\rm vis}$ (see *e.g.*, [65–67]): $c^2_{\rm eff}$ generalizes the linear relation between isotropic pressure perturbations and density perturbations, while $c^2_{\rm vis}$ modifies the neutrino anisotropic stress equation. While relativistic free-streaming species have $(c^2_{\rm eff}, c^2_{\rm vis}) = (1/3, 1/3)$, a perfect relativistic fluid would have $(c^2_{\rm eff}, c^2_{\rm vis}) = (1/3, 0)$. Other values do not necessarily refer to a concrete model, but make it possible to interpolate between these limits. *Planck* data, alone or in combination with galaxy clustering, strongly suggests $(c^2_{\rm eff}, c^2_{\rm vis}) = (1/3, 1/3)$ [68–70].

Finally, Ref. [23] (resp. [26]) shows that current data are precise enough to detect the "neutrino drag" effect mentioned in Sec. 26.2 through the measurement of the CMB peak (resp. BAO) scale. These findings show that current cosmological data are able to detect not just the average density of some relativistic relics, but also their anisotropies.

26.3.3 *Neutrino masses*

Table 26.2 shows a list of constraints on $\sum m_\nu$ obtained with several combinations of data sets. The acronyms 'Pl18' and 'BAO' have been described in the previous subsection, while 'ACT' refers to CMB observations from the Atacama Cosmology Telescope [50], 'RSD' to redshift-space distortions from the eBOSS galaxy survey [49], 'Shape' to the shape parameter of the matter power spectrum measured by the BOSS (eBOSS) galaxy redshift survey [51, 71–73], 'Lyman-α' to the one-dimensional flux power spectrum of eBOSS quasars [52], 'SN' to the Type Ia supernovae compilation of [74], 'DES-Y1' to the weak lensing and galaxy auto- and cross-correlation measured by the Dark Energy Survey (DES) using Year 1 data [75], and 'DES-Y3' for the same quantity estimated from DES Year 3 data [53].

Given that most determinations of $N_{\rm eff}$ are compatible with the standard prediction, $N_{\rm eff} = 3.044$, it is reasonable to adopt this value as a theoretical prior and to investigate neutrino mass constraints in the context of a minimal 7-parameter model, ΛCDM+$\sum m_\nu$. Under this assumption, the most robust constraints come from *Planck* 2018 temperature and polarization data alone: $\sum m_\nu < 0.26\,{\rm eV}$ (95%CL) [24]. Among the four effects of neutrino masses on the CMB spectra

described before, current bounds are dominated by the first and the third effects (modified late background evolution, and distortions of the temperature and polarization spectra through weak lensing).

Adding measurements of the BAO scale is crucial, since the determination of the angular diameter distance at small redshift allows us to break parameter degeneracies, for instance between $\sum m_\nu$ and h. The combination of Pl18[TT,TE,EE+lowE] with the most recent BAO measurements, including the eBOSS Data Release 16 (DR16), gives $\sum m_\nu < 0.13\,\mathrm{eV}$ (95%CL) [49]. Supernovae data are less constraining than BAO data for the neutrino mass determination.

Because the parameter correlation between $\sum m_\nu$ and H_0 is negative, the inclusion of DL data would tend to provide stronger bounds on neutrino masses. However, like for $N_{\rm eff}$, such bounds would not be meaningful, since they would arise from a combination of discrepant data sets. Thus, to constrain neutrino masses, it is once more crucial to understand whether the Hubble tension arises from unmodeled aspects that have no effect on the current treatment and interpretation of the datasets adopted here or new physical ingredients.

Taking the former point of view, it is interesting to add LSS data sets, sensitive also to the small-scale suppression of the matter power spectrum due to neutrino free-streaming, although most of the constraining power for current data sets comes from the constraints on the expansion history and growth-history signals [76]. The inclusion of CMB lensing data from *Planck* 18 improves the CMB-only bound only by a small amount, but the inclusion of higher resolution CMB lensing maps from ACT [50] brings the limit down to 0.12 eV. To get an even stronger bound, one can add data from the eBOSS survey, which infers the growth rate of structures from RSDs. The addition of BAO and RSD measurements from eBOSS tightens the bound down to $\sum m_\nu < 0.10\,\mathrm{eV}$ (95%CL) [49]. Further including information about the large-scale shape ('Shape') of the power spectrum, BOSS+eBOSS data alone give $\sum m_\nu < 0.40\,\mathrm{eV}$ (95%CL) with a BBN prior on ω_b, while *Planck*+BOSS+eBOSS give $\sum m_\nu < 0.082$ eV (95% CL) [51]. A similar bound arises from the most recent Lyα forest data from BOSS combined with *Planck* and BAO data, giving $\sum m_\nu < 0.087$ eV (95% CL). Such bounds already challenge the inverted hierarchy mass scheme, which predicts $\sum m_\nu \geq 0.11\,\mathrm{eV}$ (e.g., [47] and refs. therein).

It should however be noticed that DES prefers a lower σ_8 value than the *Planck* best fit, relaxing the bound to $\sum m_\nu < 0.12\,\mathrm{eV}$ (95%CL) [49] when using Year 1 data in combination with eBOSS and other datasets (Pl18+BAO+RSD+SN+DES). Using Year 3 data and a similar combination, the DES collaboration obtains $\sum m_\nu < 0.13\,\mathrm{eV}$ (95%CL) [53]. Notice however that the DES analysis adopts a theory prior $\sum m_\nu \geq 0.06$eV while other contraints only assume $\sum m_\nu \geq 0$. For a direct comparison, the combined constraint of reference [49] can be recomputed with the same theory prior and becomes $\sum m_\nu < 0.13$ eV (95%CL).

Leaving aside DL measurements, one finds that upper bounds on neutrino masses become weaker when other data are analysed in the context of extended cosmological models, but only by a small amount. Floating $N_{\rm eff}$ instead of fixing it to 3.044 has no significant impact on the neutrino mass bounds reported in the previous paragraphs. Even in the extreme case considered by Ref. [25], with 12 free cosmological parameters, one can see in Table 26.2 that the bound from *Planck* 2018 (without lensing) + BAO increases from 0.13 eV to 0.52 eV (95% CL) only. This shows that current cosmological data are precise enough to disentangle the effect of several extended cosmological parameters, and that neutrino mass bounds are becoming increasingly robust.

One should stress again that if the explanation of DL measurements requires a cosmological scenario with new – and yet unkown – physical ingredients, the current neutrino mass bounds may in principle be shifted or relaxed. However, in the absence of working scenarios that convincingly explain the Hubble tension without raising other tensions, we do not at the moment have any framework for quoting alternative mass bounds and assessing their model dependence.

26.4 Future prospects and outlook

The cosmic neutrino background has been detected indirectly at very high statistical significance. Direct detection experiments are now being planned, *e.g.*, at the Princeton Tritium Observatory for Light, Early Universe, Massive-neutrino Yield (PTOLEMY) [77]. The detection prospects crucially depend on the exact value of neutrino masses and on the enhancement of their density at the location of the Earth through gravitational clustering in the Milky Way and its sub-halos – an effect however expected to be small [78–81].

Over the past few years the upper limit on the sum of neutrino masses has become increasingly stringent, first indicating that the mass ordering is hierarchical and recently putting the inverted hierarchy under pressure and favouring the normal hierarchy (although quantitative estimates of how disfavoured the inverted hierarchy is vary depending on assumptions, see *e.g.* [44, 46, 47, 82–84]) which has consequences for planning future double beta-decay experiments. However, these bounds rely on the ΛCDM model or its most simple extensions, and thus, on the assumption that a resolution of the Hubble tension with DL measurements does not affect the modeling and interpretation of the data sets adopted here. If this is not the case, a shift of paradigm might be required, potentially leading to weaker neutrino density and mass bounds.

Neutrino mass and density bounds are expected to keep improving significantly over the next years, thanks to new LSS experiments like DESI [85], Euclid [86], LSST [87], SPHEREx [88] and SKA [89], in combinations with new CMB experiments like Simons Observatory [90], CMB-S4 [91] or LiteBird [92]. If the ΛCDM model is confirmed, and if neutrinos have standard properties, the total neutrino mass should be detected at the level of at least 3–4σ even at the minimum level allowed by oscillations. This is the conclusion reached by several independent studies, using different dataset combinations (see *e.g.*, [39, 93–98]). One should note that at the minimum level allowed by oscillations $\sum m_\nu \sim 0.06\,\mathrm{eV}$, neutrinos constitute $\sim 0.5\%$ of the Universe matter density, and their effects on the matter power spectrum is only at the 5% level, implying that exquisite control of systematic errors will be crucial to achieve the required accuracy. At this level, the information coming from the power spectrum shape is more powerful than that coming from geometrical measurements (e.g., BAO). But exploiting the shape information, especially on small, mildly non-linear or non-linear scales, requires improved understanding of the non-linear regime, and of galaxy bias for galaxy surveys. The fact that different surveys, different probes, and different data set combinations have enough statistical power to reach this level, offers a much needed redundancy and the possibility to perform consistency checks which in turns helps immensely with the control of systematic errors and in making the measurement robust. Using the entire Universe as a particle detector, the on-going and future observational efforts hold the exciting prospect to provide a measurement of the sum of neutrino masses and possibly indication of their mass hierarchy.

References

[1] A. D. Dolgov, Phys. Rept. **370**, 333 (2002), [hep-ph/0202122].

[2] J. Lesgourgues and S. Pastor, Phys. Rept. **429**, 307 (2006), [arXiv:astro-ph/0603494].

[3] S. Hannestad, Prog. Part. Nucl. Phys. **65**, 185 (2010), [arXiv:1007.0658].

[4] J. Lesgourgues *et al.*, *Neutrino Cosmology*, Cambridge University Press (2013), ISBN 978-1-108-70501-1, 978-1-139-60341-6.

[5] M. Archidiacono *et al.*, JCAP **1608**, 08, 067 (2016), [arXiv:1606.07673].

[6] L. Lancaster *et al.*, JCAP **1707**, 07, 033 (2017), [arXiv:1704.06657].

[7] I. M. Oldengott *et al.*, JCAP **1711**, 11, 027 (2017), [arXiv:1706.02123].

[8] M. Park *et al.*, Phys. Rev. D **100**, 6, 063524 (2019), [arXiv:1904.02625].

[9] C. D. Kreisch, F.-Y. Cyr-Racine and O. Doré, Phys. Rev. D **101**, 12, 123505 (2020), [arXiv:1902.00534].

[10] N. Blinov *et al.*, Phys. Rev. Lett. **123**, 19, 191102 (2019), [arXiv:1905.02727].

[11] N. Schöneberg *et al.*, Phys. Rept. **984**, 1 (2022), [arXiv:2107.10291].

[12] J. Birrell, C.-T. Yang and J. Rafelski, Nucl. Phys. **B890**, 481 (2014), [arXiv:1406.1759].

[13] G. Mangano *et al.*, Nucl. Phys. **B729**, 221 (2005), [hep-ph/0506164].

[14] E. Grohs *et al.*, Phys. Rev. **D93**, 8, 083522 (2016), [arXiv:1512.02205].

[15] P. F. de Salas and S. Pastor, JCAP **1607**, 07, 051 (2016), [arXiv:1606.06986].

[16] J. Froustey, C. Pitrou and M. C. Volpe, JCAP **12**, 015 (2020), [arXiv:2008.01074].

[17] J. J. Bennett *et al.*, JCAP **04**, 073 (2021), [arXiv:2012.02726].

[18] M. Cielo *et al.* (2023), [arXiv:2306.05460].

[19] J. Froustey, *The Universe at the MeV era : neutrino evolution and cosmological observables*, Ph.D. thesis, Institut d'Astrophysique de Paris, France, Paris, Inst. Astrophys. (2022), [arXiv:2209.06672].

[20] S. Bashinsky and U. Seljak, Phys. Rev. **D69**, 083002 (2004), [arXiv:astro-ph/0310198].

[21] Z. Hou *et al.*, Phys. Rev. **D87**, 083008 (2013), [arXiv:1104.2333].

[22] J. Lesgourgues *et al.*, *Neutrino cosmology* (Cambridge University Press, 2013).

[23] B. Follin *et al.*, Phys. Rev. Lett. **115**, 9, 091301 (2015), [arXiv:1503.07863].

[24] N. Aghanim *et al.* (Planck), Astron. Astrophys. **641**, A6 (2020), [Erratum: Astron.Astrophys. 652, C4 (2021)], [arXiv:1807.06209].

[25] E. Di Valentino, A. Melchiorri and J. Silk, JCAP **01**, 013 (2020), [arXiv:1908.01391].

[26] D. Baumann *et al.*, Nature Phys. **15**, 465 (2019), [arXiv:1803.10741].

[27] A. Lewis and A. Challinor, Phys. Rept. **429**, 1 (2006), [arXiv:astro-ph/0601594].

[28] J. Lesgourgues and S. Pastor, Adv. High Energy Phys. **2012**, 608515 (2012), [arXiv:1212.6154].

[29] Z. Hou *et al.*, Astrophys. J. **782**, 74 (2014), [arXiv:1212.6267].

[30] J. R. Bond, G. Efstathiou and J. Silk, Phys. Rev. Lett. **45**, 1980 (1980), [,61(1980)].

[31] W. Hu, D. J. Eisenstein and M. Tegmark, Phys. Rev. Lett. **80**, 5255 (1998), [arXiv:astro-ph/9712057].

[32] S. Bird, M. Viel and M. G. Haehnelt, Mon. Not. Roy. Astron. Soc. **420**, 2551 (2012), [arXiv:1109.4416].

[33] C. Wagner, L. Verde and R. Jimenez, Astrophys. J. **752**, L31 (2012), [arXiv:1203.5342].

[34] C. J. Todero Peixoto, V. de Souza and P. L. Biermann, JCAP **1507**, 07, 042 (2015), [arXiv:1502.00305].

[35] J. Brandbyge and S. Hannestad, JCAP **1710**, 10, 015 (2017), [arXiv:1706.00025].

[36] J. Adamek, R. Durrer and M. Kunz, JCAP **1711**, 11, 004 (2017), [arXiv:1707.06938].

[37] M. Archidiacono *et al.*, JCAP **1702**, 02, 052 (2017), [arXiv:1610.09852].

[38] A. Liu *et al.*, Phys. Rev. **D93**, 4, 043013 (2016), [arXiv:1509.08463].

[39] R. Allison *et al.*, Phys. Rev. **D92**, 12, 123535 (2015), [arXiv:1509.07471].

[40] J. Lesgourgues, S. Pastor and L. Perotto, Phys. Rev. **D70**, 045016 (2004), [hep-ph/0403296].

[41] A. Slosar, Phys. Rev. **D73**, 123501 (2006), [arXiv:astro-ph/0602133].

[42] R. Jimenez *et al.*, JCAP **1005**, 035 (2010), [arXiv:1003.5918].

[43] R. Jimenez, C. P. Garay and L. Verde, Phys. Dark Univ. **15**, 31 (2017), [arXiv:1602.08430].

[44] A. F. Heavens and E. Sellentin, JCAP **04**, 047 (2018), [arXiv:1802.09450].

[45] M. Archidiacono, S. Hannestad and J. Lesgourgues, JCAP **09**, 021 (2020), [arXiv:2003.03354].

[46] F. Capozzi *et al.*, Phys. Rev. D **104**, 8, 083031 (2021), [arXiv:2107.00532].

[47] R. Jimenez *et al.*, JCAP **09**, 006 (2022), [arXiv:2203.14247].

[48] S. Gariazzo, O. Mena and T. Schwetz, Phys. Dark Univ. **40**, 101226 (2023), [arXiv:2302.14159].

[49] S. Alam *et al.* (eBOSS), Phys. Rev. D **103**, 8, 083533 (2021), [arXiv:2007.08991].

[50] M. S. Madhavacheril *et al.* (ACT) (2023), [arXiv:2304.05203].

[51] S. Brieden, H. Gil-Marín and L. Verde, JCAP **08**, 08, 024 (2022), [arXiv:2204.11868].

[52] N. Palanque-Delabrouille *et al.*, JCAP **04**, 038 (2020), [arXiv:1911.09073].

[53] T. M. C. Abbott *et al.* (DES), Phys. Rev. D **105**, 2, 023520 (2022), [arXiv:2105.13549].

[54] E. di Valentino, S. Gariazzo and O. Mena, Phys. Rev. D **106**, 4, 043540 (2022), [arXiv:2207.05167].

[55] A. G. Riess *et al.*, Astrophys. J. Lett. **934**, 1, L7 (2022), [arXiv:2112.04510].

[56] Y. S. Murakami *et al.* (2023), [arXiv:2306.00070].

[57] E. Di Valentino *et al.* (2023), [arXiv:2305.12989].

[58] J. L. Bernal, L. Verde and A. G. Riess, JCAP **1610**, 10, 019 (2016), [arXiv:1607.05617].

[59] L. Verde, T. Treu and A. G. Riess, Nature Astron. **3**, 891 (2019), [arXiv:1907.10625].

[60] J. L. Bernal *et al.*, Phys. Rev. D **103**, 10, 103533 (2021), [arXiv:2102.05066].

[61] E. Di Valentino *et al.*, Class. Quant. Grav. **38**, 15, 153001 (2021), [arXiv:2103.01183].

[62] E. Abdalla *et al.*, JHEAp **34**, 49 (2022), [arXiv:2203.06142].

[63] J. F. Beacom, N. F. Bell and S. Dodelson, Phys. Rev. Lett. **93**, 121302 (2004), [arXiv:astro-ph/0404585].

[64] A. G. Riess *et al.*, Astrophys. J. Lett. **908**, 1, L6 (2021), [arXiv:2012.08534].

[65] W. Hu, Astrophys. J. **506**, 485 (1998), [arXiv:astro-ph/9801234].

[66] W. Hu *et al.*, Phys. Rev. **D59**, 023512 (1999), [arXiv:astro-ph/9806362].

[67] M. Gerbino, E. Di Valentino and N. Said, Phys. Rev. **D88**, 6, 063538 (2013), [arXiv:1304.7400].

[68] B. Audren *et al.*, JCAP **1503**, 036 (2015), [arXiv:1412.5948].

[69] P. A. R. Ade *et al.* (Planck), Astron. Astrophys. **594**, A13 (2016), [arXiv:1502.01589].

[70] S. Kumar, R. C. Nunes and P. Yadav, JCAP **09**, 060 (2022), [arXiv:2205.04292].

[71] T. Simon, P. Zhang and V. Poulin, JCAP **07**, 041 (2023), [arXiv:2210.14931].

[72] A. Semenaite *et al.*, Mon. Not. Roy. Astron. Soc. **512**, 4, 5657 (2022), [arXiv:2111.03156].

[73] C. Moretti *et al.* (2023), [arXiv:2306.09275].

[74] D. M. Scolnic *et al.*, Astrophys. J. **859**, 2, 101 (2018), [arXiv:1710.00845].

[75] T. M. C. Abbott *et al.* (DES), Phys. Rev. D **98**, 4, 043526 (2018), [arXiv:1708.01530].

[76] A. Boyle and E. Komatsu, JCAP **03**, 035 (2018), [arXiv:1712.01857].

[77] S. Betts *et al.*, in "Proceedings, 2013 Community Summer Study on the Future of U.S. Particle Physics: Snowmass on the Mississippi (CSS2013): Minneapolis, MN, USA, July 29-August 6, 2013," (2013), [arXiv:1307.4738], URL `http://www.slac.stanford.edu/econf/C1307292/docs/submittedArxivFiles/1307.4738.pdf`.

[78] A. Ringwald and Y. Y. Y. Wong, JCAP **0412**, 005 (2004), [hep-ph/0408241].

[79] F. Villaescusa-Navarro *et al.*, JCAP **1303**, 019 (2013), [arXiv:1212.4855].

[80] P. F. de Salas *et al.*, JCAP **1709**, 09, 034 (2017), [arXiv:1706.09850].

[81] M. Bauer and J. D. Shergold, JCAP **01**, 003 (2023), [arXiv:2207.12413].

[82] F. Simpson *et al.*, JCAP **1706**, 06, 029 (2017), [arXiv:1703.03425].

[83] S. Hannestad and T. Schwetz, JCAP **1611**, 11, 035 (2016), [arXiv:1606.04691].

[84] S. Roy Choudhury and S. Hannestad, JCAP **07**, 037 (2020), [arXiv:1907.12598].

[85] A. Aghamousa *et al.* (DESI) (2016), [arXiv:1611.00036].

[86] R. Laureijs *et al.* (EUCLID) (2011), [arXiv:1110.3193].

[87] Paul A. Abell *et al.*, LSST Science and LSST Project Collaborations, `http://lss.fnal.gov/archive/test-tm/2000/fermilab-tm -2495-a.pdf` (2009) `arXiv:0912.0201`.

[88] J. Bock and SPHEREx Science Team, in "American Astronomical Society Meeting Abstracts #231," volume 231 of *American Astronomical Society Meeting Abstracts*, 354.21 (2018).

[89] `http://www.skatelescope.org`.

[90] P. Ade *et al.* (Simons Observatory), JCAP **02**, 056 (2019), [arXiv:1808.07445].

[91] K. N. Abazajian *et al.* (CMB-S4) (2016), [arXiv:1610.02743].

[92] M. Hazumi *et al.*, J. Low Temp. Phys. **194**, 5-6, 443 (2019).

[93] C. Carbone *et al.*, JCAP **1103**, 030 (2011), [arXiv:1012.2868].

[94] J. Hamann, S. Hannestad and Y. Y. Y. Wong, JCAP **1211**, 052 (2012), [arXiv:1209.1043].

[95] B. Audren *et al.*, JCAP **1301**, 026 (2013), [arXiv:1210.2194].

[96] R. Pearson and O. Zahn, Phys. Rev. **D89**, 4, 043516 (2014), [arXiv:1311.0905].

[97] F. Villaescusa-Navarro, P. Bull and M. Viel, Astrophys. J. **814**, 2, 146 (2015), [arXiv:1507.05102].

[98] T. Brinckmann *et al.*, JCAP **1901**, 059 (2019), [arXiv:1808.05955].